An electron paramagnetic resonance study of $Pr_{0.6}Ca_{0.4}MnO_3$ across the charge-ordering transition

2000 J. Phys.: Condens. Matter 12 6919

(http://iopscience.iop.org/0953-8984/12/30/319)

J. Phys.: Condens. Matter **12** (2000) 6919–6926. Printed in the UK PII: S0953-8984(00)13479-4

An electron paramagnetic resonance study of $Pr_{0.6}Ca_{0.4}MnO_3$ across the charge-ordering transition

Rajeev Gupta†, Janhavi P Joshi†, S V Bhat†, A K Sood† and C N R Rao‡

† Department of Physics, Indian Institute of Science, Bangalore 560 012, India

‡ CSIR Centre for Excellence in Chemistry, Jawaharlal Nehru Centre for Advanced Scientific Research, Jakkur PO, Bangalore 560 064, India

Received 25 April 2000, in final form 23 June 2000

Abstract. We report the first electron paramagnetic resonance studies of single crystals and powders of $Pr_{0.6}Ca_{0.4}MnO_3$ in the 300–4.2 K range, covering the charge-ordering transition (T_{co}) at ∼240 K and antiferromagnetic transition (T_N) at ∼170 K. The asymmetry parameter for the Dysonian single-crystal spectra shows an anomalous increase at T_{co}. Below T_{co} the g-value increases continuously, suggesting a gradual strengthening of the orbital ordering. The linewidth undergoes a sudden increase at T_{co} and continues to increase down to T_N. The intensity increases as the temperature is decreased until T_{co} is reached, due to the renormalization of the magnetic susceptibility arising from the build-up of ferromagnetic correlations.

1. Introduction

Recent investigations of rare-earth manganites and related systems exhibiting colossal magnetoresistance has led to the discovery of interesting phenomena related to charge, spin and orbital ordering in these materials [1]. Phase diagrams of these systems as functions of doping and temperature are therefore very interesting, showing regimes of varied magnetic and electrical properties. These manganites of general composition $A_{1-x}A'_xMnO_3$ where A is a trivalent rare-earth ion (e.g. La, Pr, Nd) and A′ is a divalent ion (e.g. Ca, Sr, Pb) show a rich phase diagram [2] depending on the tolerance factor and the amount of doping x which, in turn, controls the ratio of Mn^{3+} to Mn^{4+}. The end members of this series, i.e. those with $x = 0$ and $x = 1$, are A-type and G-type antiferromagnetic insulators (AFI), respectively. For $0.17 < x < 0.5$ the system undergoes a metal-to-insulator (MI) transition as the temperature is increased. This MI transition also coincides with the magnetic transition from the ferromagnetic to the paramagnetic state. The electronic properties of these systems are understood qualitatively in terms of the Zener's double-exchange (DEX) interaction [3–5]. In DEX there is a strong Hund's coupling between the three t_{2g} electrons, whose spins are parallel and constitute a core spin of 3/2, and the lone e_g spin. This e_g electron can hop from one Mn^{3+} site to an adjacent Mn^{4+} site via the intermediate oxygen when the core spins are parallel, which also implies that metallicity coincides with ferromagnetism. To explain the resistivity data, Millis *et al* [6] invoked the localization of charge carriers above T_c due to polaron formation. In the case of systems where the weighted-average A-site cation radius is small, the system also shows charge ordering (CO), i.e. real-space ordering of Mn^{3+} and Mn^{4+} ions, as a function of temperature. The CO state becomes stable when the repulsive Coulomb interaction between carriers is dominant over the kinetic energy. In such cases there is a strong

0953-8984/00/306919+08$30.00

competition between the double-exchange interaction which favours ferromagnetism and CO which favours antiferromagnetism. The smaller size of the A-site cation leads to a deviation in the Mn–O–Mn bond angle from 180°, resulting in a lowering of the transfer integral. This in turn implies a lower bandwidth of the e_g electron and hence higher electronic correlations in the system. The stability of the CO state depends on the commensurability of the carrier concentration with the periodicity of the crystal lattice; it is stable for $x = 0.5$.

$Pr_{1-x}Ca_xMnO_3$ shows a rich phase diagram as a function of doping and temperature and has been well studied using a variety of probes like resistivity [7], magnetization [8], neutron diffraction studies [9–12] and transmission electron microscopy [13]. For $x = 0.4$, the sample is insulating at all temperatures in zero field. The resistivity changes by more than six orders of magnitude from 300 K to 50 K. There is a perceptible change in slope at around $T_{co} \sim 240$ K signifying the onset of charge ordering. In the temperature range $T > T_{co}$ (240 K) the system is a paramagnetic insulator. In dc magnetic susceptibility, a large peak is observed at T_{co} followed by a relatively small peak at T_N. The peak at T_{co} is attributed to ferromagnetic correlations [10]. The system further undergoes a transition at 170 K to a CE-type AFI. The pseudo-CE-type structure for $x < 0.5$ is different to the CE structure present in systems with $x = 0.5$. In this so-called 'pseudo-CE' structure, the zigzag ferromagnetic (FM) chains in the ab-plane are FM aligned along the c-axis [10]. This is unlike the case for the CE structure where the layers in the ab-plane are aligned antiferromagnetically along the c-axis. Further lowering of the temperature below 50 K leads to another transition which can be understood either as a canted antiferromagnetic state [11, 12] or as a mixture of ferromagnetic domains or clusters in an antiferromagnetic background.

In this paper we report our EPR study of single crystals as well as powders of $Pr_{0.6}Ca_{0.4}MnO_3$ as a function of temperature from 300 K to 4.2 K. Although several EPR studies on the manganites across the metal–insulator transition have been reported recently [14–21], to our knowledge, there has been no study across the CO transition. The dynamics of spins in the charge-ordered state as studied by means of EPR is expected to throw some light on the controversial magnetic structure between the charge-ordering transition and the Néel temperature.

2. Experimental details

The single crystal used for the experiment was prepared by the float-zone technique and characterized using dc magnetic susceptibility, which shows a large peak at 240 K (T_{co}) and a relatively small peak at 170 K (T_N). The measurements on single crystals were done with the magnetic field parallel to the (100) axis. Powder of the material was dispersed in paraffin wax for study. The EPR measurements were carried out at 9.2 GHz (X band) with a Bruker spectrometer (model 200 D) equipped with an Oxford Instruments continuous-flow cryostat (model ESR 900), with a temperature accuracy of ±2 K.

3. Results and discussion

Figure 1 shows the EPR spectra at a few temperatures in the range 300 K to 180 K recorded in the heating run for a single crystal (figure 1(a)) and a powder sample (figure 1(b)). The ESR signal could be observed only above 180 K. The observed signals are very broad. The spectra from the single crystal are Dysonian in shape and were fitted (solid lines in figure 1(a)) to a functional form similar to the one used by Ivanshin *et al* [21] for $La_{1-x}Sr_xMnO_3$. The field

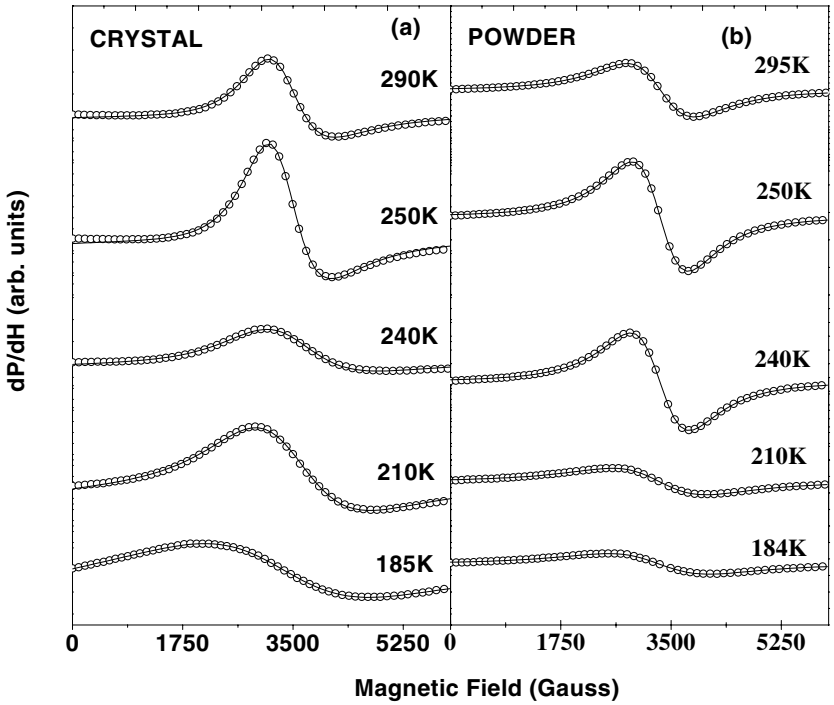

Figure 1. Derivative spectra of $Pr_{0.6}Ca_{0.4}MnO_3$ for (a) single crystal and (b) a powder sample at a few selected temperatures. The signal from DPPH has been subtracted in (b). The solid lines show the Dysonian and Lorentzian fits to the crystal and powder sample data respectively.

derivative of the power absorbed given by

$$\frac{\mathrm{d}P}{\mathrm{d}H} \propto \frac{\mathrm{d}}{\mathrm{d}H}\left(\frac{\Delta H + \alpha(H - H_{res})}{(H - H_{res})^2 + \Delta H^2} + \frac{\Delta H + \alpha(H + H_{res})}{(H + H_{res})^2 + \Delta H^2}\right) \tag{1}$$

incorporates responses to both of the circular components of the exciting linearly polarized microwave field. The above equation also includes both absorption and dispersion. α, the asymmetry parameter, is a measure of the dispersion-to-absorption ratio. The spectra from powder samples are symmetrical and were well fitted with Lorentzians as shown in figure 1(b).

Careful EPR measurements on doped manganites by Causa *et al* [17] and Lofland *et al* [20] show that both Mn^{3+} and Mn^{4+} contribute to the EPR signal. The bottleneck model used by Shengelaya *et al* [19] also shows that the EPR intensity is proportional to the total susceptibility of the Mn^{4+} and Mn^{3+} spins. We will first discuss our results on the temperature dependence of the EPR lineshape parameters of single crystals.

Figure 2 shows the temperature dependence of the lineshape parameters of the signals obtained by fitting to equation (1). Figure 2(a) shows the temperature dependence of the linewidth (ΔH). The linewidth decreases as the temperature is lowered from 300 K down to just above T_{co} and then nearly doubles across the charge-ordering transition. This increase is somewhat similar to that observed [19] in $LaCaMnO_3$ across the paramagnetic insulator-to-ferromagnetic metal transition, thereby implying a build-up of spin correlations at T_{co}. The increase in linewidth above T_{co} can be interpreted in terms of spin–lattice relaxation or even as an opening up of the 'bottleneck' as the temperature is raised [19, 20]. Figure 2(c) shows

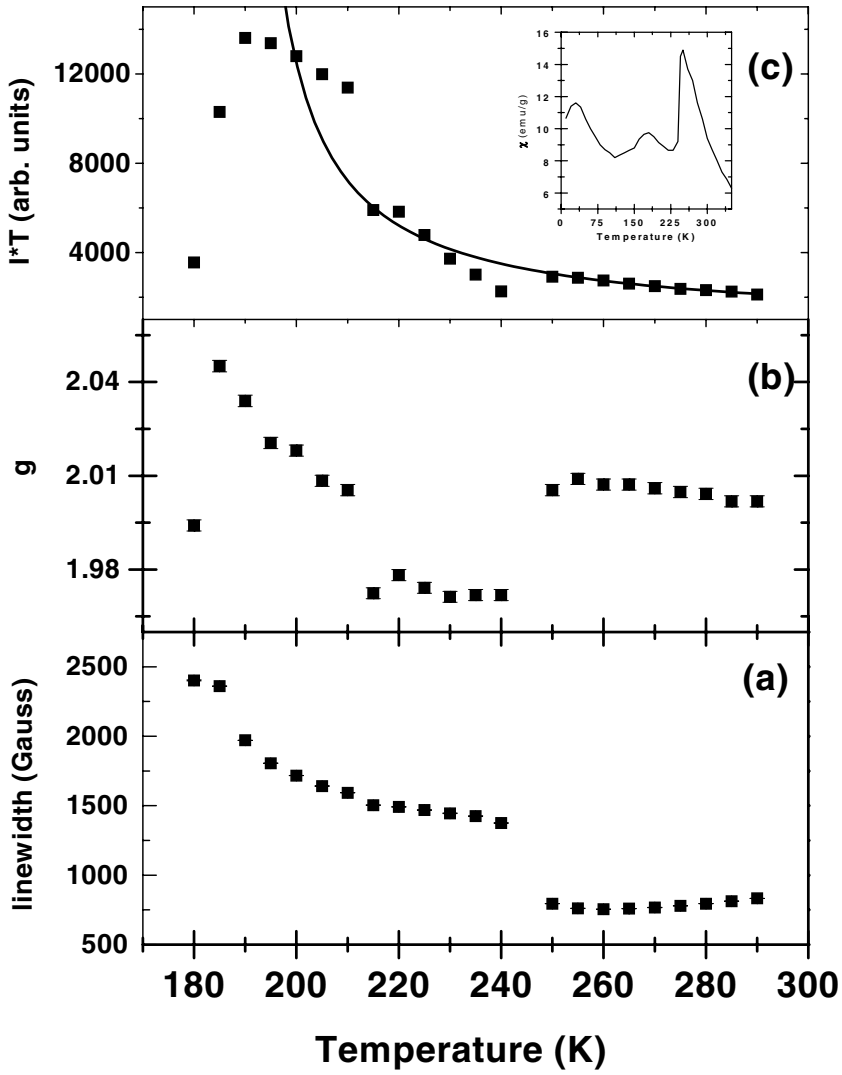

Figure 2. Variation of the lineshape parameters—linewidth, g and intensity as functions of temperature for the single-crystal data obtained by fitting to equation (1). The solid line in (c) shows the fit for $T > T_{co}$ to equation (2) and (3) as discussed in the text. The inset shows the temperature variation of the dc magnetic susceptibility.

the variation of the integrated intensity as a function of temperature. We have tried to analyse the temperature dependence of the intensity in terms of the bottleneck model [19, 25]. In this picture, the EPR signal originates from both Mn^{4+} and Mn^{3+} ions and the intensity is proportional to the total susceptibility. Here the spin–spin relaxation rates for the exchange-coupled Mn^{3+} and Mn^{4+} ions are much larger than the spin–lattice relaxation rates. In this regime the ferromagnetic correlations will renormalize the spin susceptibility given by [19]:

$$I \propto \chi_{total} = \chi_s + \chi_\sigma \tag{2}$$

where χ_s and χ_σ are the renormalized static susceptibilities and are given by

$$\chi_s = \chi_s^0 \frac{1 + \lambda\chi_\sigma^0}{1 - \lambda^2\chi_\sigma^0\chi_s^0} \qquad \chi_\sigma = \chi_\sigma^0 \frac{1 + \lambda\chi_s^0}{1 - \lambda^2\chi_\sigma^0\chi_s^0} \tag{3}$$

where χ_s^0 is the bare spin susceptibility of Mn^{4+} and χ_σ^0 is the bare spin susceptibility of Mn^{3+}. The parameter $\lambda = zJ/Ng_sg_\sigma\mu_B^2$, where J is the exchange coupling constant for exchange between Mn^{4+} and Mn^{3+} spins, g_s (g_σ) is the g-factor of Mn^{4+} (Mn^{3+}) ions, N is the number of spins per cm^3, z is the number of nearest neighbours and μ_B is the Bohr magneton. We can get an estimate of J by fitting equations (2) and (3) to the data in figure 2(c)—taking $g_s = g_\sigma = 2$, $z = 6$ and assuming that the bare susceptibility of Mn^{4+} ions is given by the Curie law $\chi_s^0 = C_s/T$ while that of Mn^{3+} follows a Curie–Weiss law: $C_\sigma/(T - \Theta)$, where Θ, the negative Curie–Weiss temperature, is taken to be the same as that for undoped $LaMnO_3$ ($\Theta = -100$ K). The solid line shows the fit to the intensity data above T_{co} yielding a qualitative estimate of $J \sim 154$ K. This value is of the same order of magnitude as the value obtained for J ($\sim$70 K) for doped manganites from EPR measurements [19] and neutron scattering [26] and Brillouin scattering experiments [27]. At this stage we would also like to point out that though all spins contribute to the EPR intensity, the temperature dependence is qualitatively different from the dc susceptibility data (as shown in the inset of figure 2(c)). This could be due to the fact that the resistivity of the sample increases by two orders of magnitude in the temperature regime of 300–180 K which will enhance the penetration depth, and hence the volume of the sample 'seen' by the microwave field is changing with temperature. Figure 2(b) shows the temperature variation of the g-value. Since internal-field effects can influence the single-crystal data, we will focus our attention on the temperature variation of g only in the powder data.

The 'asymmetry parameter' α of the signals, obtained from single-crystal data, is shown in figure 3. The ratio remains practically constant from 300 K to T_{co} where it discontinuously increases. Further cooling results in a decrease of the α-value, as is to be expected from the decrease in conductivity at lower temperatures (the resistivity [22] shown in the inset of figure 3). The discontinuous *increase* of α at T_{co} is interesting because normally one would have expected a decrease following the decrease in conductivity. However, as shown by Dyson [23] and Feher and Kip [24], the value of α depends also on the ratio of the time T_D taken by the electrons to diffuse through the skin depth and the spin–spin relaxation time T_2. The sudden increase in α therefore indicates a sudden dip in the value of T_D/T_2. This implies that the value of T_2 increases at T_{co} to offset the increase in T_D due to decrease in the conductivity. However, this is contrary to the observed increase in the linewidth at T_{co}. At present, we do not have a satisfactory explanation of this result.

Figure 4 shows the temperature dependence of the lineshape parameters for the powder sample extracted by fitting the derivative of the Lorentzian function yielding the temperature dependence of the linewidth (ΔH), resonance field (H_0) and area under the curve. Figure 4(b) shows the temperature dependence of the g-factor, estimated from the resonance field. In all the earlier EPR reports on manganites, the value of g was observed to be close to or less than that for a free electron (=2.0023). Earlier EPR studies on Mn^{3+} and Mn^{4+} dilutely doped in diamagnetic hosts have given [28] $g \sim 1.98$. However, our experiments give a g-value higher than that for the free electrons for all temperatures. A speck of DPPH ($g = 2.0036$) was used as a g-marker and the centre resonance field was obtained from the fit to the Lorentzian. This procedure gives confidence in our measurements of the temperature dependence of g. Since the internal-field effects are expected to average out in powdered samples, we believe that the increase in g for $T < T_{co}$ is intrinsic in nature. One possible reason for this is the changes in the spin–orbit coupling. It is known that $g_{eff} = g[1 \pm \kappa/\Delta]$, where the

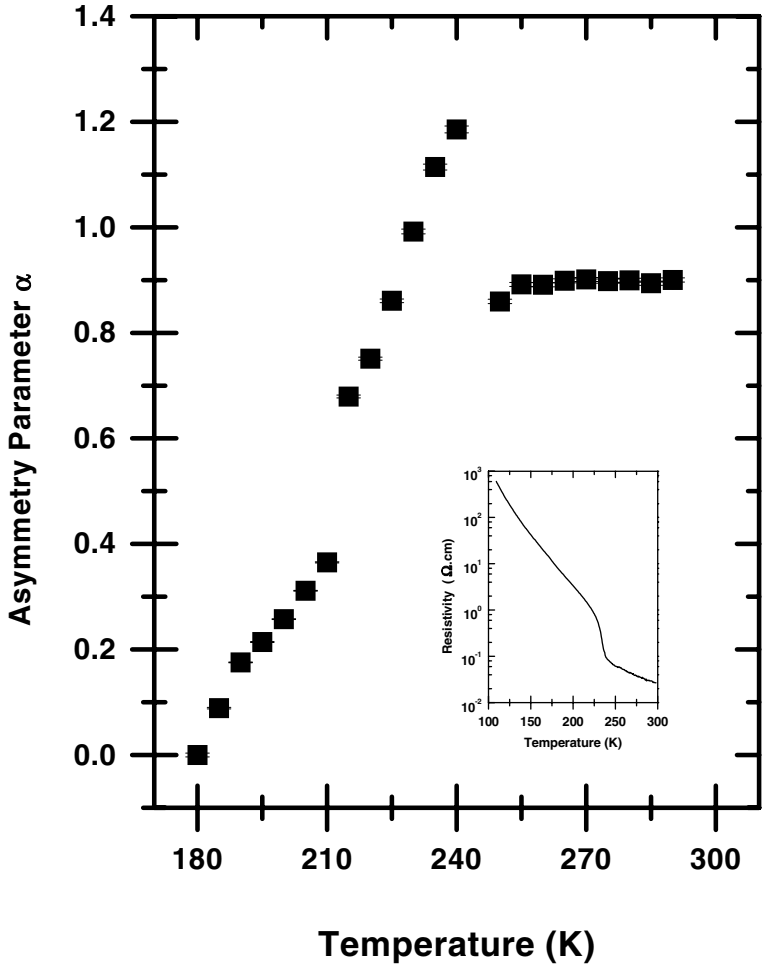

Figure 3. Variation of the asymmetry parameter α as a function of temperature for single-crystal data. The inset shows the temperature dependence of the resistivity (taken from reference [22]).

spin–orbit interaction energy is $\kappa \vec{L} \cdot \vec{S}$ and Δ is the appropriate crystal-field splitting [29]. A recent transmission electron microscopy study [13] of $Pr_{0.5}Ca_{0.5}MnO_3$ has shown that the incommensurate-to-commensurate charge ordering is coincident with the paramagnetic-to-antiferromagnetic transition at 180 K. The physical picture is that for $T_N < T < T_{co}$, orbital ordering is partial, in spite of the complete charge ordering. This orbital ordering builds up and is complete at T_N. Therefore for $T < T_{co}$ a gradual build-up of the orbital ordering can change the spin–orbit coupling as well as the crystal-field parameters and hence can lead to an increase in the value of g as the temperature is lowered. This may also be the reason for the sign of the g-shift with respect to the free-electron g, which is opposite to that expected for Mn^{3+} and Mn^{4+} ions (d shells that are less than half-filled). It will be very interesting to calculate the value of g theoretically, incorporating orbital ordering. Figure 4(a) shows the temperature variation of the full width at half-maximum of the Lorentzian, ΔH. For $T > T_{co}$, the width decreases linearly as the temperature is lowered from 300 to 240 K, similarly to that observed in single-crystal data. Below T_{co} down to 180 K, the width increases significantly

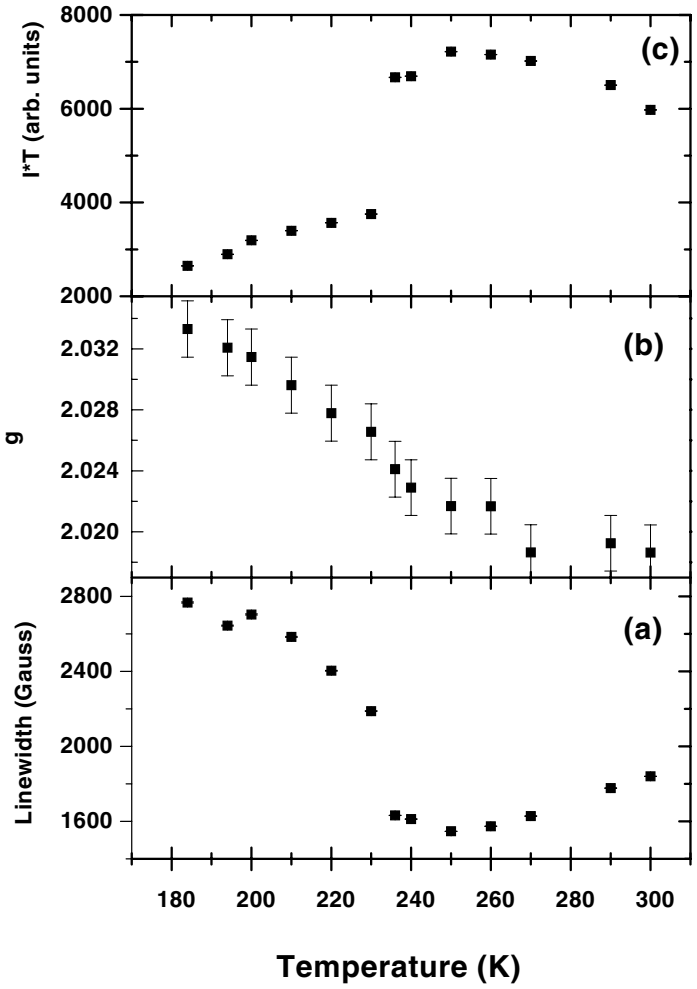

Figure 4. Lineshape parameters for the powder sample—linewidth, g and intensity as functions of temperature obtained by fitting the spectra to a Lorentzian profile.

(by almost a factor of 2). It is remarkable that the width increases sharply from ∼1600 G at 240 K to ∼2200 G at 228 K. This sharp increase can be due to magnetic fluctuations which are also responsible for the peak in the dc magnetic susceptibility. The further increase in ΔH as temperature is lowered can arise due to build-up of magnetic correlations preceding the transition to the long-range antiferromagnetic ordering at 170 K. Figure 4(c) shows the temperature dependence of the intensity which is qualitatively similar to that of single-crystal data.

4. Summary

In summary, we have reported for the first time EPR measurements on charge-ordered $Pr_{0.6}Ca_{0.4}MnO_3$. The lineshape parameters reveal a rich temperature dependence across T_{co} as well as at lower temperatures approaching T_N. The intensity variation above T_{co} is considered to be due to the renormalization of spin susceptibility due to ferromagnetic (FM) correlations. Such FM correlations in the paramagnetic insulating phase have been invoked to explain the origin of the peak in magnetic susceptibility near T_{co} and of dynamical spin fluctuations above

T_c in doped manganites [30, 31]. The formation of magnetic polarons to localize the carriers has been suggested by Varma [32]. The value of the exchange coupling constant J is estimated to be about 154 K. The fluctuations in the magnetic correlations near the transition temperatures lead to a large increase in the linewidth. The temperature dependence of the g-factor suggests a need to carry out theoretical calculations of g invoking orbital ordering.

Acknowledgments

SVB and AKS thank the Department of Science and Technology for financial assistance. We thank Professor B S Shastry for his suggestion of doing the EPR experiments and for useful discussions. JPJ thanks CSIR for financial support.

References

[1] Rao C N R and Raveau B (ed) 1998 *Colossal Magnetoresistance, Charge Ordering and Related Properties of Manganese Oxides* (Singapore: World Scientific)
[2] Woodward P M, Vogt T, Cox D E, Arulraj A, Rao C N R, Karen P and Chetham A K 1998 *Chem. Mater.* **10** 3652
[3] Zener C 1951 *Phys. Rev.* **82** 403
[4] Anderson P W and Hasegawa 1955 *Phys. Rev.* **100** 675
[5] de Gennes P G 1960 *Phys. Rev.* **118** 141
[6] Millis A J, Littlewood P B and Shraiman B I 1995 *Phys. Rev. Lett.* **74** 5144
[7] Tomioka Y, Asamitsu A, Kuwahara H, Moritomo Y and Tokura Y 1996 *Phys. Rev.* B **53** R1689
[8] Lees M R *et al* 1995 *Phys. Rev.* B **52** R14 303
[9] Yoshozawa H *et al* 1995 *Phys. Rev.* B **52** R13 148
[10] Cox D E, Radaelli P G, Marezio M and Cheong S W 1998 *Phys. Rev.* B **57** 3305
[11] Jirak Z, Krupicka S, Nekvasil V, Pollert E, Villeneuve G and Zounova F 1980 *J. Magn. Magn. Mater.* **15–18** 519
[12] Jirak Z, Krupicka S, Simsa Z, Dlouha M and Vratislav S 1985 *J. Magn. Magn. Mater.* **53** 153
[13] Mori S *et al* 1999 *Phys. Rev.* B **59** 13 573
[14] Huber D L *et al* 1999 *Phys. Rev.* B **60** 12 155
[15] Oseroff S B *et al* 1996 *Phys. Rev.* B **53** 6521
[16] Rivadulla F *et al* 1999 *Phys. Rev.* B **60** 11 922
[17] Causa M T *et al* 1998 *Phys. Rev.* B **58** 3233
[18] Tovar M *et al* 1999 *Phys. Rev.* B **60** 10 199
[19] Shengelaya A, Zhao G, Keller H and Muller K A 1996 *Phys. Rev. Lett.* **77** 5296
Shengelaya A *et al* 2000 *Phys. Rev.* B **61** 5888
[20] Lofland S E *et al* 1997 *Phys. Lett.* A **233** 476
[21] Ivanshin V A *et al* 2000 *Phys. Rev.* B **61** 6213
[22] Guha A *et al* 2000 unpublished
[23] Dyson F J 1955 *Phys. Rev.* **98** 349
[24] Feher G and Kip A F 1955 *Phys. Rev.* **98** 337
[25] Kochelaev B I, Kan L, Elschner B and Elschner S 1994 *Phys. Rev.* B **49** 13 106
[26] Dai P *et al* 2000 *Phys. Rev.* B **61** 9553
[27] Murugavel P *et al* 2000 unpublished
[28] Pilbrow J 1990 *Transition Ion Electron Paramagnetic Resonance* (Oxford: Oxford Science) p 421
[29] Kittel C 1991 *Introduction to Solid State Physics* (New York: Wiley) p 420
[30] Lynn J W *et al* 1996 *Phys. Rev. Lett.* **76** 4046
[31] De Teresa J M *et al* 1997 *Nature* **386** 256
[32] Varma C M 1996 *Phys. Rev.* B **54** 7328